

Nanosprings

D. N. McIlroy,^{a)} D. Zhang, and Y. Kranov

Department of Physics, Engineering and Physics Building, University of Idaho, Moscow, Idaho 83844-0903

M. Grant Norton

School of Mechanical and Materials Engineering, Washington State University, Pullman, Washington 99164-2920

(Received 13 April 2001; accepted for publication 16 July 2001)

The transition from linear to helical growth of amorphous boron carbide nanowires has been examined with high-resolution transmission electron microscopy. Based on the observed changes of the iron catalyst at the transition point from linear to helical growth, a model of helical growth of solid nanowires has been developed based on the work of adhesion of the metallic catalyst to the tip of the nanowire. This model demonstrates that contact angle anisotropy at the catalyst/wire interface drives helical growth. The anisotropy is introduced when the radius of the droplet (R) exceeds the radius of the nanowire (ρ), and the center of mass of the metal droplet is displaced laterally from the central axis of the nanowire. © 2001 American Institute of Physics. [DOI: 10.1063/1.1400079]

Research and development on the growth and properties of solid and molecular (nanotubes) nanowires has increased steadily over the last decade, largely due to their potential applications in nanoelectronics, nanomechanics, and flat-panel displays.¹ It has been shown that nano- and micron-scale wires grow in a variety of configurations ranging from straight²⁻⁵ to helical.⁶⁻¹³ While the growth of straight nanowires and nanotubes²⁻⁵ is well understood and a model for the helical growth of carbon nanotubes has been proposed,¹² a model to describe the helical growth of nanowires, which are solid as opposed to hollow (nanotubes), is lacking. Here, we report the growth of helical boron carbide nanowires, as well as present a model for their growth.

Briefly, the synthesis of nanotubes¹⁴ and nanowires²⁻⁵ on surfaces can be promoted through the introduction of a metallic catalyst. This growth mechanism is known as the vapor-liquid-solid (VLS) growth mode, first described by Wagner and Ellis.¹⁵ In VLS growth, a liquid droplet of a metal or a metal eutectic resides on a substrate. The droplet absorbs the building block material for the growth of the nanowire from the surrounding vapor. Once the concentration reaches supersaturation within the droplet, the excess material is secreted out the base of the droplet to the liquid/solid interface, thereby forming the wire beneath the droplet.

Displayed in Fig. 1 is a transmission electron microscope (TEM) image of a boron carbide (BC) nanospring grown on a silicon substrate by the technique of plasma-enhanced chemical vapor deposition (PECVD), where Fe was the catalyst.^{2,3} The nanospring is 60 nm in diameter and approximately 1 μm in length, with a pitch of 27 nm and a wire diameter, proper, of 20 nm. The diameters of the BC nanosprings in this sample ranged from 20 to 30 nm, with pitches from 31 to 43 nm and nanowire diameters from 20 to 30 nm. The sample consisted of linear (90%) and helical (10%) nanowires. Using high-resolution TEM, the structure of the BC nanosprings and the straight nanowires have been

determined to be amorphous. This is consistent with the cited cases of helical growth of solid wires.⁷⁻⁹

In Fig. 2 we present TEM images of the transition region from straight to helical growth of two BC nanowires, where at the transition a fraction of the Fe catalyst has become embedded at the end of the straight section of the nanowire. A total of eight transitions of the type displayed in Fig. 2

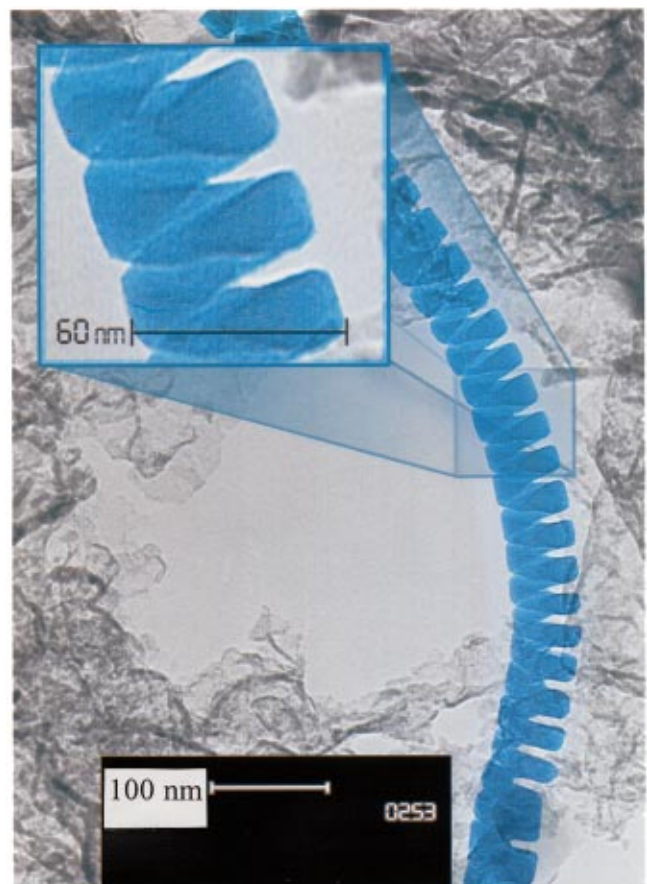


FIG. 1. (Color) Bright-field transmission electron microscope image of an amorphous boron carbide nanospring that has been highlighted for contrast. The inset is a blown-up view of the nanospring.

^{a)}Electronic mail: dmcilroy@uidaho.edu

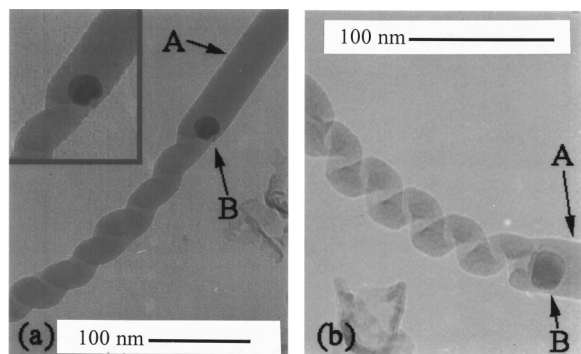


FIG. 2. Bright-field transmission electron microscope images of amorphous boron carbide nanosprings. The inset in (a) is a close-up view of the Fe catalyst embedded in the nanowire. The arrows labeled A identify the straight nanowires, while the arrows labeled B identify the Fe droplets (catalyst).

were observed. The diameter of the straight nanowire in Fig. 2(a) [Fig. 2(b)] is 41 nm (39 nm), the diameter of the nanowire forming the nanospring is 28 nm (22 nm), the pitch of the nanospring is 38 nm (35 nm), and the diameter of the embedded Fe catalyst is 24 nm (26 nm). Note, for carbon nanotube growth the diameter of the nanotube can exceed the diameter of the catalyst and the catalyst can reside at the base, the tip, or within the nanotube,¹² while for VLS growth of solid nanowires the diameter of the catalyst cannot be less than the diameter of the nanowire and must reside at the tip of the nanowire. Consequently, the order of growth in Fig. 2 is from straight to helical. The smaller diameters of the embedded Fe catalysts relative to the diameters of the straight nanowires, in conjunction with the continuation of nanowire growth in the helical mode, indicate that portions of the catalysts were ejected from the parent Fe droplets at the points of encapsulation. Note that for both nanosprings the encased Fe droplet is offset to the edge of the nanowire and that helical growth originates at the edges of the straight nanowires. This indicates that the secondary droplets were ejected at the edges of the nanowires, which may account for the notch in the Fe droplet (inset) in Fig. 2(a) and the slight asymmetry in the droplet in Fig. 2(b).

The diameters of the ejected Fe droplets can be calculated from the dimensions of the straight nanowires and the helical nanowires in Fig. 2. First, we assume that the diameter of the parent droplet was equivalent to the diameter of the straight wire. Second, we assume a spherical geometry for the ejected droplet, which is supported by the observed spherical shape of the encased Fe droplets in Fig. 2 and by TEM images of straight BC nanowires capped with spherical Fe particles. Therefore, the diameters of the ejected Fe droplets that formed the nanosprings were 19 nm [Fig. 2(a)] and 17 nm [Fig. 2(b)], respectively. The ratios of the radii of the ejected droplets (R) to the radii of the nanowires (ρ) forming the nanosprings are 1.36 [Fig. 2(a)] and 1.54 [Fig. 2(b)], respectively.

In order to model the VLS growth of BC nanosprings, the dynamics of the catalyst must be determined. The modulated stress-strain model proposed by Amelinckx *et al.*¹² to describe the helical growth of carbon nanotubes suggested that asymmetry arises from variations in the velocity of the growth front about the perimeter of the carbon nanotube due

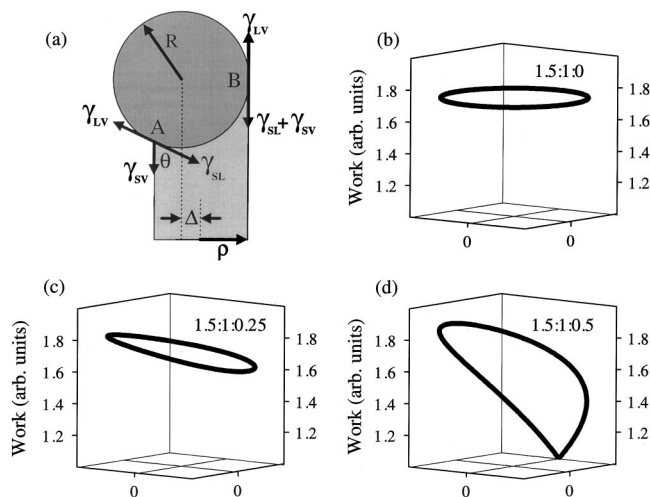


FIG. 3. (a) Diagram depicting an iron droplet (catalyst) of radius R atop a boron carbide nanowire of radius ρ , (b) the work of adhesion [$W_A(R:\rho:\Delta)$] of a metal droplet (catalyst) to a nanowire for $(R:\rho:\Delta)=(1.5:1:0)$, (c) $=(1.5:1:0.25)$, and (d) $=(1.5:1:0.5)$, where all of the variables have been normalized to the radius of the nanowire.

to competition between opposing growth planes. This model is inadequate for describing the helical growth of solid amorphous nanowires because it cannot explain the behavior observed in Fig. 2 and ignores interactions between the catalyst and the nanowire, i.e., R cannot be less than ρ , etc., as well as fails to identify the physical mechanism inducing anisotropy. However, the proposed anisotropy in the velocity of the growth front in this model is obviously correct and applicable to the helical growth of solid amorphous nanowires. Consequently, it is the mechanism behind the anisotropy that we will address.

We propose that the asymmetry of the growth front velocity for the BC nanosprings is due to contact angle anisotropy (CAA) at the Fe droplet-nanowire interface. The trajectory of the droplet can be quantified by examining the work needed to shear the droplet from the tip of the BC nanowire, which is related to the surface tensions (γ) between the liquid-vapor (γ_{LV}), solid-vapor (γ_{SV}), and solid-liquid (γ_{SL}) interfaces. Figure 3(a) depicts a cross-sectional view of an Fe droplet (catalyst) atop a BC nanowire, where R is the radius of the Fe droplet, ρ is the radius of the nanowire, and Δ is the displacement of the center of mass of the droplet from the central axis of the nanowire. CAA is introduced by the displacement Δ of the Fe droplet. At the interface labeled A in Fig. 3(a), the interfacial surface tensions γ_{LV} and γ_{SL} are antiparallel, while γ_{SV} is rotated by an angle θ out of the plane containing γ_{LV} and γ_{SL} . However, at interface B the interfacial surface tensions lie within the same plane, where γ_{SV} is parallel to γ_{SL} . Consequently, there is a nonzero torque on the Fe droplet that will cause the droplet to shear from the BC nanowire.

The work required to shear the Fe droplet from the BC nanowire, referred to as the work of adhesion (W_A), can be quantified in terms of the interfacial surface tensions¹⁶ and is defined by the following relationship:

$$\begin{aligned} W_A &= \gamma_{SV} + \gamma_{SL} - \gamma_{LV} \\ &= \gamma_{SV} + \gamma_{SL} - (\gamma_{SL} + \gamma_{SV} \cos \theta) \\ &= \gamma_{SV}(1 - \cos \theta). \end{aligned}$$

Consequently, the work of adhesion depends on the angle between the surface tensions γ_{SV} and γ_{SL} . At interface A [Fig. 3(a)] the interaction between the droplet and the nanowire is a nonwetting interaction, while at interface B the droplet is in a condition of spontaneous wetting, i.e., $\theta=0$. The work of adhesion at the perimeter of the droplet–wire interface for a number of geometries are displayed in Fig. 3. For all of the calculations we have chosen the ratio of the radius (R) of the droplet to the radius (ρ) of the nanowire to be 1.5, i.e., the ratio observed for the nanospring in Fig. 2(b). If the center of mass of the droplet coincides with the central axis of the nanowire, the work of adhesion [Fig. 3(b)] is uniform about the perimeter of the droplet/nanowire interface and, therefore, precludes asymmetric growth, i.e., helical growth. However, by offsetting the droplet from the axis of the nanowire, CAA is introduced and the work of adhesion [Fig. 3(c)] is no longer symmetric, where the minimum [Fig. 3(c)] corresponds to the closest approach of the interface to the edge of the droplet. In Fig. 3(d) the work of adhesion has been plotted for the conditions depicted in Fig. 3(a), where the offset has been increased to half of the radius of the nanowire, thereby maximizing CAA. In addition to the expected asymmetry, a well-defined cusp in W_A is introduced at interface B [Fig. 3(a)], where the minimum of W_A is a factor of 2 less than that of the centered droplet [Fig. 3(b)]. Note that by systematically increasing the radius of the droplet the work of adhesion will be returned to the symmetric configuration displayed in Fig. 3(b).

The significance of the asymmetry in the work of adhesion in Fig. 3(c) is as follows. The probability of a boron or carbon atom diffusing through the Fe droplet and attaching itself to a point at the droplet–nanowire interface will be a function of the energy needed to break a droplet–nanowire bond, less the energy gained by making a new B or C bond to the nanowire. The amount of energy needed to accomplish this will depend thermodynamically on the work of adhesion, where the probability of attachment of a B or C atom at the droplet–nanowire interface is higher at the points of lower work of adhesion. So, the growth rate velocity at interface B (v_B) will be greater than the growth rate velocity at interface A (v_A), thereby creating the asymmetry necessary to curl the trajectory of the droplet back upon the nanowire. Because the cusp in Fig. 3(d) is a point of instability, a small lateral perturbation will produce the precession necessary to drive the droplet into a spiral trajectory that can be described using the trajectory mechanics described by Amelinckx *et al.*¹² for

helical carbon nanotubes. Based on the analysis of the work of adhesion (W_A) of the metal droplet (catalyst) to the nanowire, we have concluded that the optimal geometry for promoting spiral growth is achieved when the ratio $R/\rho \approx 1.5$ and the extreme edge of the droplet coincides with the edge of the nanowire, as depicted in Fig. 3(a), which is consistent with Fig. 2 and the corresponding ratios of R/ρ .

The observed growth of amorphous boron carbide nanosprings, in conjunction with the CAA model, illustrates the importance of the catalyst for promoting nanowire growth as well as the affect of its trajectory on the geometry of the BC nanowire. Furthermore, since the CAA model for nanospring growth is material independent, provided the wires are amorphous, it can be universally used to describe the growth of all types of nano- and micron-sized springs, regardless of their composition.

One of the authors (D.N.M.) would like to thank Professor George Patsakos for his useful input and acknowledge the support of the Office of Naval Research, Physical Sciences S&T Division (Grant N00014-99-1-0772).

- ¹K. W. Wong, X. T. Zhou, F. C. K. Au, H. L. Lai, C. S. Lee, and S. T. Lee, *Appl. Phys. Lett.* **75**, 2918 (1999).
- ²D. Zhang, D. N. McIlroy, Y. Geng, and M. G. Norton, *J. Mater. Sci. Lett.* **18**, 349 (1999).
- ³D. N. McIlroy, D. Zhang, R. M. Cohen, J. Wharton, Y. Geng, M. G. Norton, G. De Stasio, B. Gilbert, L. Perfetti, J. H. Streiff, B. Broocks, and J. L. McHale, *Phys. Rev. B* **60**, 4874 (1999).
- ⁴D. Zhou and S. Seraphin, *Chem. Phys. Lett.* **222**, 232 (1994).
- ⁵A. M. Morales and C. M. Lieber, *Science* **279**, 208 (1998).
- ⁶Y. H. Tang, Y. F. Zhang, N. Wang, C. S. Lee, X. D. Han, I. Bello, and S. T. Lee, *J. Appl. Phys.* **85**, 7981 (1999).
- ⁷S. Motojima, S. Ueno, T. Hattori, and K. Goto, *Appl. Phys. Lett.* **54**, 1001 (1989).
- ⁸S. Motojima, Y. Itoh, S. Asakura, and H. Iwanaga, *J. Mater. Sci.* **30**, 5049 (1995).
- ⁹K. M. Kadish and R. S. Ruoff, *Electrochem. Soc. Proc.* **97-14**, 875 (1997).
- ¹⁰R. T. K. Baker, P. S. Harris, and S. Terry, *Nature (London)* **253**, 37 (1975).
- ¹¹V. Ivanov, J. B. Nagy, Ph. Lambin, A. Lucas, X. B. Zhang, X. F. Zhang, D. Bernaerts, G. Van Tendeloo, S. Amelinckx, and J. Van Landuyt, *Chem. Phys. Lett.* **223**, 329 (1994).
- ¹²S. Amelinckx, X. B. Zhang, D. Bernaerts, X. F. Zhang, V. Ivanov, and J. B. Nagy, *Science* **265**, 635 (1994).
- ¹³A. Volodin, M. Ahlskog, E. Seynaeve, C. Van Haesendonck, A. Fonseca, and J. B. Nagy, *Phys. Rev. Lett.* **84**, 3342 (2000).
- ¹⁴G. T. Kim, E. S. Choi, D. C. Kim, D. S. Suh, Y. W. Park, K. Liu, G. Duesberg, and S. Roth, *Phys. Rev. B* **58**, 16064 (1998).
- ¹⁵R. S. Wagner and W. C. Ellis, *Appl. Phys. Lett.* **4**, 89 (1964).
- ¹⁶R. S. Wagner, *Whisker Technology* (Wiley Interscience, New York, 1970), p. 257.